JPET Fast Forward. Published on December 17, 2020 as DOI: 10.1124/jpet.120.000096
This article has not been copyedited and formatted. The final version may differ from this version.

Title page

Different anti-oxidative and anti-apoptotic effects of piceatannol and resveratrol.

Ryusuke Hosoda, Hiroki Hamada, Daisuke Uesugi, Naotoshi Iwahara, Iyori Nojima, Yoshiyuki Horio, Atsushi Kuno

Department of Pharmacology, School of Medicine, Sapporo Medical University (R.H., N.I., I.N., Y.H., A.K.), Sapporo, Japan

Department of Life Science, Faculty of Science, Okayama University of Science (H.H., D.U.), Okayama, Japan

JPET Fast Forward. Published on December 17, 2020 as DOI: 10.1124/jpet.120.000096
This article has not been copyedited and formatted. The final version may differ from this version.

Running title page

a) Running title:

Comparison of piceatannol with resveratrol.

b) Address for correspondence

Atsushi Kuno, MD, PhD

Department of Pharmacology

Sapporo Medical University School of Medicine

South-1, West-17, Chuo-ku

Sapporo 060-8556, Japan

Phone: +81-11-611-2111

Fax: +81-11-612-5861

Email: kuno@sapmed.ac.jp

c) Number of text page: 36

Number of tables: 0

Number of figures: 7

Number of references: 48

Numbers of words in the Abstract: 249

Number of words in the Introduction: 787

Number of words in the Discussion: 1,124

d) Abbreviations: 7-AAD, 7-amino-actinomycin D; DPPH, 2, 2'-diphenyl-1-picrylhydrazyl; ESI-MS, electrospray ionization mass spectrometry; FoxO, forkhead box O transcription factor; GAPDH, glyceraldehyde-3-phosphate dehydrogenase; GCLM, Glutamate-Cysteine

JPET Fast Forward. Published on December 17, 2020 as DOI: 10.1124/jpet.120.000096
This article has not been copyedited and formatted. The final version may differ from this version.

Ligase Modifier Subunit; HO1, heme oxygenase 1; Keap1, Kelch-like ECH-associated protein 1; NAC, N-acetyl-L-cysteine; NQO1, NAD(P)H:quinone oxidereductase 1; NRF2, nuclear factor erythroid 2-related factor 2; PBS, phosphate-buffered saline; PIC, piceatannol; RT-qPCR, quantitative reverse transcription-polymerase chain reaction; ROS, reactive oxygen species; RSV, resveratrol; SIRT1, sirtuin 1; SOD2, superoxide dismutase 2.

e) Recommended section assignment: Cellular and Molecular

JPET Fast Forward. Published on December 17, 2020 as DOI: 10.1124/jpet.120.000096
This article has not been copyedited and formatted. The final version may differ from this version.

Abstract

Resveratrol affords protection against reactive oxygen species (ROS)-related diseases via activation of SIRT1, an NAD^+-dependent deacetylase. However, the low bioavailability of resveratrol limits its therapeutic applications. Since piceatannol is a hydroxyl analogue of resveratrol with higher bioavailability, it could be an alternative to resveratrol. In this study, we compared the cytotoxicity, anti-oxidative activity, and mechanisms of cytoprotection of piceatannol with those of resveratrol. In C2C12 cells incubated with piceatannol, ESI-MS analysis showed that piceatannol was present in the intracellular fraction. A high concentration (50 μM) of piceatannol, but not resveratrol, induced mitochondrial depolarization and apoptosis. However, piceatannol at 10 μM inhibited the increase in mitochondrial ROS level induced by antimycin A, and this ROS reduction was greater than that by resveratrol. The reduction in H_2O_2-induced ROS by piceatannol was also greater than that by resveratrol or vitamin C. Piceatannol reduced antimycin A-induced apoptosis more than did resveratrol. SIRT1 knockdown abolished the anti-apoptotic activity of resveratrol, whereas it blocked only half of the anti-apoptotic activity of piceatannol. Piceatannol, but not resveratrol, induced heme oxygenase-1 (HO1) expression, which was blocked by knockdown of the transcription factor NRF2, but not by SIRT1 knockdown. HO1 knockdown partially blocked the reduction of ROS by piceatannol. Furthermore, the anti-apoptotic action of piceatannol was abolished by HO1 knockdown. Our results suggest that the therapeutic dose of piceatannol protects cells against mitochondrial ROS more than does resveratrol via SIRT1- and NRF2/HO1-dependent mechanisms. The activation of NRF2/HO1 could be an advantage of piceatannol compared with resveratrol for cytoprotection.

JPET Fast Forward. Published on December 17, 2020 as DOI: 10.1124/jpet.120.000096
This article has not been copyedited and formatted. The final version may differ from this version.

Significance Statement

We showed here that piceatannol and resveratrol were different in cytotoxicity, oxidant scavenging activities, and mechanisms of cytoprotection. Protection by piceatannol against apoptosis induced by reactive oxygen species was superior to that by resveratrol. In addition to the SIRT1-dependent pathway, piceatannol exerted NRF2/HO1-mediated anti-oxidative and anti-apoptotic effects, which could be an advantage of piceatannol compared with resveratrol.

JPET Fast Forward. Published on December 17, 2020 as DOI: 10.1124/jpet.120.000096
This article has not been copyedited and formatted. The final version may differ from this version.

Introduction

Piceatannol (3,3',4,5'-trans-tetrahydroxystilbene; PIC) and resveratrol (3,4',5-trans-trihydroxystilbene; RSV) are natural stilbenes found in grape skins and have therapeutic potentials against cancers, cardiovascular diseases, inflammation, hypercholesterolemia, and obesity (Bonkowski and Sinclair, 2016; Piotrowska et al., 2012; Salehi et al., 2018; Seyed et al., 2016). PIC has high apoptosis-inducing ability for tumor cells (Piotrowska et al., 2012; Seyed et al., 2016). On the other hand, since PIC possesses one extra hydroxyl residue compared with RSV (Figure 1A), PIC provides higher anti-oxidation activity than that of resveratrol (Rhayem et al., 2008; Sato et al., 2014; Sueishi et al., 2017). PIC has been shown to protect cells from toxicities of amyloid beta and the lipid peroxide product 4-hydroxynonenal, both of which increase the production of cellular reactive oxygen species (ROS) (Jang et al., 2009; Kim et al., 2007). In addition to increasing the production of ROS, these compounds also activate ROS-independent mechanisms such as a caspase cascade and calcium influx in cells. Thus, the effects of PIC on cell death induced only by high levels of ROS have not been studied in detail.

Both PIC and RSV activate SIRT1, an NAD^+-dependent protein deacetylase (Howitz et al., 2003). SIRT1 is a mammalian homologue of yeast Sir2, which prolongs lifespan when overexpressed in yeast (Kaeberlein et al., 1999). Activation of SIRT1 reduces cellular oxidative stress, cell death and inflammation and promotes mitochondrial biogenesis and lipid metabolism (Horio et al., 2011). Deacetylation of forkhead box O transcription factors (FoxOs) and peroxisome proliferator-activated receptor gamma coactivator 1-alpha by SIRT1 leads to their activation to induce the expression of anti-oxidative enzymes such as superoxide dismutase 2 (SOD2) (Pan and Finkel, 2017). Although RSV itself is an anti-oxidant, our previous data suggest that induction of anti-oxidative enzymes mediated via SIRT1 activation

is the main mechanism of the anti-oxidative action of RSV (Hori et al., 2013; Hosoda et al., 2013; Tanno et al., 2010).

RSV and PIC have also been reported to activate nuclear factor erythroid 2-related factor 2 (NRF2) to induce anti-oxidative action (Hao et al., 2013; Lee et al., 2010; Perez-Leal et al., 2017). NRF2 is a transcription factor that promotes the expression of anti-oxidative genes such as heme oxygenase-1 (HO1) and NAD(P)H:quinone oxidereductase 1 (NQO1) (Cuadrado et al., 2019). In cells without stress, activity of NRF2 is repressed by Keap1, which forms a complex with NRF2, leading to ubiquitin-mediated degradation of NRF2. ROS-induced release of NRF2 from Keap1 causes stabilization and nuclear translocation of NRF2, leading to its transcriptional activation. Acetylation/deacetylation of NRF2 also regulates NRF2 activity. It has been reported that acetylation of NRF2 by p300/CREB-binding protein augments its DNA binding (Sun et al., 2009). There are opposite reports regarding roles of SIRT1 in NRF2 activity. One study showed that SIRT1 attenuates transcription activity of NRF2 via its deacetylation (Kawai et al., 2011), whereas another study showed that SIRT1 increases nuclear NRF2 protein level and its transcription activity (Huang et al., 2013).

Pathological ROS are derived from various sources including the electron transport chain in mitochondria, especially in organs rich in mitochondria (Balaban et al., 2005), cytochrome P450 in the liver (Veith and Moorthy, 2018), and NADPH oxidases in the cardiovascular systems (Zhang et al., 2020). Among them, mitochondrial ROS are liberated into the cytoplasm and the nucleus and are implicated in various pathological conditions such as muscular diseases and neurodegenerative diseases (Balaban et al., 2005; Bock and Tait, 2020). Besides SOD2 induction, SIRT1 activation by RSV induces autophagy/mitophagy to attenuate mitochondrial oxidative stress (Lee et al., 2012; Morselli et al., 2011; Sebori et al., 2018). In a model of culture cells, it has been shown that RSV decreases cellular ROS and

JPET Fast Forward. Published on December 17, 2020 as DOI: 10.1124/jpet.120.000096
This article has not been copyedited and formatted. The final version may differ from this version.

apoptosis induced by antimycin A, a product of Streptomyces that inhibits mitochondrial electron transport chain complex III, via SIRT1 (Hori et al., 2013; Tanno et al., 2010). In contrast, it is not known whether PIC protects cells from cytotoxicity induced by ROS generated from mitochondria.

We have shown that RSV has the potential for treatment of ROS-related diseases including Duchenne muscular dystrophy and heart failure (Kuno et al., 2018; Sebori et al., 2018; Tanno et al., 2010). However, it has been pointed out that a weak point of RSV is its low bioavailability when orally administered (Almeida et al., 2009). Since PIC is an analogue of RSV and has been reported to have higher bioavailability than that of RSV (Setoguchi et al., 2014), PIC could be an alternative candidate for treatment of ROS-related diseases. However, it remains unclear whether the cytotoxicity and anti-oxidative properties of PIC are different from those of RSV.

In the present study, we compared the cytotoxicity, anti-mitochondrial ROS activity, and involvement of SIRT1 and NRF2 in the anti-apoptotic function of PIC with those of RSV in C2C12 myoblasts.

Materials and Methods

Reagents

PIC was obtained from Tokyo Kasei (Tokyo, Japan). RSV, antimycin A, hydrogen peroxide (H_2O_2), and N-acetyl-L-cysteine (NAC) were purchased from FUJIFILM Wako Pure Chemicals (Osaka, Japan). Vitamin C was obtained from Kanto Chemical (Tokyo, Japan). MitoSOX Red was purchased from Thermo Fisher Scientific (Waltham, MA, USA). Hoechst33342 was obtained from Dojindo (Kumamoto, Japan).

Mass spectrometry

JPET Fast Forward. Published on December 17, 2020 as DOI: 10.1124/jpet.120.000096
This article has not been copyedited and formatted. The final version may differ from this version.

Electrospray ionization mass spectrometry (ESI-MS) was performed with an Q Exactive Plus (Thermo Fischer Scientific) in negative ionization mode (ESI-) with a methanol carrier solution at a flow rate of 0.5 µl/min and with an injection volume of 2 µl.

Measurement of DPPH radical-scavenging activity

The 2,2-diphenyl-1-picrylhydrazyl (DPPH) radical-scavenging activity was measured as previously reported (Morales and Jimenez-Perez, 2001) with a slight modification. Briefly, 500 µl of a test sample in water was mixed with the same volume of 0.15 mM DPPH dissolved in 99.5% ethanol. The mixture was shaken for 30 minutes at room temperature, and then absorbance of the mixture was measured at 517 nm. Data are shown as percent inhibition according to the formula $[Abs_{(control)} - Abs_{(sample)} / Abs_{(control)}] \times 100$. The 50% inhibitory concentration (IC50) was calculated by $10^{(Log(A/B)x(50-C)/(D-C)+Log(B)}$, where A is the concentration of the test compound directly above 50% inhibition, B is the concentration of the test compound directly below 50% inhibition, C is the percent inhibition at B, and D is the percent inhibition at A.

Cell culture

C2C12 myoblasts were cultured in Dulbecco's modified Eagle's medium (DMEM, Wako Pure Chemical) with 4.5 g/L D-glucose supplemented with 1% antibiotic-antimycotic mixed stock solution (Nacalai Tesque, Kyoto, Japan) and 10% fetal bovine serum. The culture medium was switched to serum-free DMEM to eliminate cytoprotective factors in serum and to obtain reproducible cytotoxicity in experiments for cell death, mitochondrial membrane potential, mitochondrial ROS, and gene expression analyses.

Detection of intracellular and extracellular piceatannol

JPET Fast Forward. Published on December 17, 2020 as DOI: 10.1124/jpet.120.000096
This article has not been copyedited and formatted. The final version may differ from this version.

C2C12 cells in a 10-cm dish were incubated with or without the culture medium containing 100 μM PIC for 1 h. After removal of the culture medium, the cells were washed twice with PBS and lysed with 0.5 mL of CelLytic M Cell Lysis Reagent (Sigma-Aldrich). The cell lysates were then sonicated and centrifuged. The supernatant fraction was mixed with an equal volume of ethyl acetate and shaken vigorously for 30 minutes at room temperature. The ethyl acetate layer, which contained PIC, was isolated and then evaporated. PIC in the culture medium (10 mL) was also extracted with ethyl acetate. Dried samples were stored at -80°C. The samples were dissolved in 100 μl of methanol and examined by ESI-MS. Experiments were independently carried out at least three times.

Immunoblot analysis

C2C12 cells were lysed with CelLytic M Cell Lysis Reagent with 1% protease inhibitor cocktail (Nacalai Tesque) and centrifuged at 10,000 g for 10 minutes at 4°C. The supernatant fractions were analyzed by immunoblot analysis as described previously (Hosoda et al., 2013). Protein concentration was measured with the Protein Quantification Kit-Rapid (Dojindo) and equal protein amounts per lane (7 μg) were analyzed using the following antibodies: rabbit polyclonal anti-SIRT1 (Sakamoto et al., 2004) (1:1,000) and mouse monoclonal anti-tubulin (Sigma-Aldrich, T5168, 1:10,000) antibodies.

Apoptosis-inducing effects of PIC and RSV

C2C12 cells were treated with a vehicle (dimethyl sulfoxide) and various concentrations of RSV or PIC in serum-free DMEM for 4 h. Apoptotic cell death was analyzed by nuclear condensation and by flow cytometry. Cell nuclei were stained with Hoechst33342 (1:2,000) and observed by fluorescence microscopy. The percentage of cells with condensed nuclei was averaged from five fields of each treatment. For analysis by flow cytometry, cells were

JPET Fast Forward. Published on December 17, 2020 as DOI: 10.1124/jpet.120.000096
This article has not been copyedited and formatted. The final version may differ from this version.

stained using the Muse™ Annexin V & Dead Cell Kit (Millipore). The cells were fractionated into four fractions according to the manufacturer's protocol: non-apoptotic cells, Annexin V (-) and 7-Amino-Actinomycin D (7-AAD) (-); early apoptotic cells, Annexin V (+) and 7-AAD (-); late stage apoptotic and dead cells, Annexin V (+) and 7-AAD (+); and necrotic cells, Annexin V (-) and 7-AAD (+). Three independent experiments were carried out.

Assay for mitochondrial membrane depolarization

C2C12 cells were treated with dimethyl sulfoxide as a vehicle and various concentrations of RSV or PIC in serum-free DMEM for 4 h. Mitochondrial membrane potential and dead cells were analyzed by flow cytometry with the Muse® MitoPotential Kit (Millipore). Cells were fractionated into four fractions according to the manufacturer's protocol: live cells, MitoPotential Dye (+) and 7-AAD (-); depolarized live cells, MitoPotential Dye (-) and 7-AAD (-); depolarized and dead cells, MitoPotential Dye (-) and 7-AAD (+); and dead cells, MitoPotential Dye (+) and 7-AAD (+). Three independent experiments were carried out.

RNA analysis

Total RNA isolation from cultured cells and reverse transcriptase reaction were performed as described previously (Hori et al., 2013; Hosoda et al., 2013). Quantitative PCR was performed in StepOne (Applied Biosystems, Foster City, CA) using TaqMan Universal Master Mix II with UNG (Applied Biosystems) and TaqMan Gene Expression Assays for SOD2 (Mm00449726_m1), Myogenin (Mm00446194_m1), MyoD (Mm00440387_m1) , MYH4 (Mm01332541_m1), and GAPDH (Mm99999915_g1). For analyses of mouse SIRT1, catalase, HO1, NQO1, GCLM, and β-actin, GoTaq qPCR Master Mix (Promega) with the following oligonucleotide primers was used: 5'-GAC GCT GTG GCA GAT TGT TA-3' and 5'-GGA ATC CCA CAG GAG ACA GA-3' for SIRT1, 5'-GGA GGC GGG AAC CCA

JPET Fast Forward. Published on December 17, 2020 as DOI: 10.1124/jpet.120.000096
This article has not been copyedited and formatted. The final version may differ from this version.

ATA G-3' and 5'-GTG TGC CAT CTC GTC AGT GAA-3' for mouse catalase, 5'-GTC AAG CAC AGG GTG ACA GA-3' and 5'-CTG CAG CTC CTC AAA CAG CT-3' for mouse HO1, 5'-ACA TGA ACG TCA TTC TCT GG-3' and 5'-ACC AGT TGA GGT TCT AAG AC-3' for mouse NQO1, 5'-TGT GTG ATG CCA CCA GAT TG-3' and 5'-ATG CTT TCT TGA AGA GCT TCC T-3' for mouse GCLM, and 5'-CTG GCT CCT AGC ACC ATG AAG AT-3' and 5'-GGT GGA CAG TGA GGC CAG GAT-3' for mouse β-actin. All assays were performed in duplicate and by the standard curve method using serial cDNA dilution. β-actin or GAPDH was used as an internal control. Experiments were independently carried out at least three times.

Effects of PIC and RSV on the level of mitochondrial ROS induced by antimycin A or hydrogen peroxide

C2C12 cells were treated with the vehicle, 30 μM RSV, or 30 μM PIC in serum-free DMEM for 4 h and were further incubated with 45 μM antimycin A for 4 h to generate mitochondrial ROS. The cells were stained with MitoSOX Red (Thermo Fischer Scientific) to analyze the level of mitochondrial ROS according to the manufacturer's protocol, and red fluorescence was monitored using fluorescence microscopy. We also examined the effect of RSV, PIC, vitamin C or NAC on MitoSOX Red fluorescence in cells treated with 250 μM H_2O_2 for 1 h. Cells were pretreated with the vehicle (DMSO), 10 μM RSV, 10 μM PIC, 10 μM vitamin C, or 10 μM NAC for 24 h and were then co-incubated with the vehicle or H_2O_2. All images were captured under the same conditions, and the fluorescence intensity was quantified by Image-J Software (NIH). The average fluorescence intensity was obtained from 5~6 fields for each experiment, and then the data from three independent experiments were analyzed.

Effects of PIC and RSV on necrotic cell death induced by mitochondrial oxidative stress

JPET Fast Forward. Published on December 17, 2020 as DOI: 10.1124/jpet.120.000096
This article has not been copyedited and formatted. The final version may differ from this version.

C2C12 cells were treated with the vehicle, 30 μM RSV, or 30 μM PIC in serum-free DMEM for 4 h, and then 100 μM antimycin A was added to the medium to induce necrosis. After 45 min, cells that had died from necrosis were analyzed by the Muse™ Cell Analyzer with Muse™ Count and Viability Kit (Millipore) according to the manufacturer's protocol.

Transfection of siRNA

C2C12 cells were transfected with small interfering RNAs (siRNAs, 50 nM) for SIRT1 (SASI_Mm01_00105675, Sigma Aldrich), NRF2 (SASI_mM01_00013-0750), HO1 (SASI_Mm01_0015-9368) or control siRNA (SIC-001, Sigma Aldrich) by using Lipofectamine RNAiMAX Transfection Reagent (Thermo Fisher Scientific) according to the manufacturer's instructions. Cell death, MitoSOX Red, and mRNA levels were examined at 48 h after siRNA transfection.

Anti-apoptotic effects of PIC and RSV

Twenty-four hours after siRNA transfection, the cells were treated with the vehicle, 10 μM RSV, or 10 μM PIC in serum-free DMEM for 24 h and were then treated with 30 μM antimycin A for 4 h to induce apoptosis in the presence of the vehicle, RSV, or PIC. The cells were fixed with 4% paraformaldehyde and cell nuclei were stained by Hoechst 33342 (1:2,000 dilution). Apoptotic cells were determined by nuclear condensation. The percentage of cells with condensed nuclei was determined from five fields in each experiment, and the data from three independent experiments were analyzed.

Myotube differentiation of C2C12 myoblasts

For the differentiation, C2C12 cells were cultured in DMEM with 1.0 g/L D-glucose (FUJIFILM Wako Pure Chemicals) containing 2% horse serum (Thermo Fisher Scientific) for

JPET Fast Forward. Published on December 17, 2020 as DOI: 10.1124/jpet.120.000096
This article has not been copyedited and formatted. The final version may differ from this version.

1 week as previously reported (Fujiwara et al., 2019). During differentiation, cells were co-incubated with the vehicle, 10 μM RSV, or 10 μM PIC.

Statistical analysis

The data are expressed as means ± standard deviations. Comparisons between multiple groups were performed by one-way and two-way analyses of variance followed by a post-hoc Student-Neuman-Keuls test. Differences were considered significant if the P-value was less than 0.05. All analyses were carried out using SigmaStat (Systat).

Results

Higher reducing activity of PIC in vitro

PIC, a hydroxylated analogue of RSV, is expected to have a higher reducing ability than that of RSV. We compared the capacities of PIC and RSV to scavenge DPPH, a hydrogen acceptor. The DPPH-scavenging capacity of PIC was greater than that of RSV (Figure 1B). The concentrations of PIC and RSV required for 50% of the maximal DPPH-scavenging activity were approximately 18 and 81 μM, respectively. Thus, the DPPH-scavenging activity of PIC was 4.5-fold higher than that of RSV.

Entry of PIC into cells

We previously reported that resveratrol-4'-O-β-D-glucoside (4'G-RSV), a glycosyl RSV, exerts a cytoprotective function against ROS, although 4'G-RSV itself does not enter cells. In fact, 4'G-RSV is firstly deglycosylated and is converted to RSV in the extracellular space, and then RSV enters cells and affords cytoprotection (Hosoda et al., 2013). We examined whether PIC directly enters cells. ESI-MS analysis showed a peak of PIC (m/z 243) in a sample from a medium containing 100 μM PIC (Supplemental Figure 1A). When cells were

JPET Fast Forward. Published on December 17, 2020 as DOI: 10.1124/jpet.120.000096
This article has not been copyedited and formatted. The final version may differ from this version.

treated with a medium without PIC, extracellular (medium) and intracellular fractions did not show such peaks (Supplemental Figure 1B). After C2C12 cells had been treated with 100 μM PIC for 1 h, extracellular and intracellular fractions were analyzed. PIC (m/z 243) was present in the extracellular fraction as well as in the intracellular fraction (Supplemental Figure 1C). Additional peaks did not appear in the extracellular and intracellular fractions (Supplemental Figure 1C). The peak for PIC was not detected in the intracellular fraction isolated from cells harvested after incubation with PIC for 1 min (Supplemental Figure 1D).

Mitochondrial depolarization by PIC but not by RSV

Both PIC and RSV have apoptosis-inducing activity for tumor cells (Piotrowska et al., 2012; Salehi et al., 2018; Seyed et al., 2016). It has been shown that PIC induced depolarization of the mitochondrial membrane potential and apoptosis of a lymphoma cell line in a concentration-dependent manner with a half-maximum concentration of 25 μM (Wieder et al., 2001). We compared the effects of PIC and RSV on mitochondrial membrane potential and cell death in non-tumor C2C12 cells. After incubation with various concentrations of PIC or RSV under a serum-free condition, the cells were stained with MitoPotential Dye and 7-AAD (Figure 2). Live cells exclude 7-AAD, a high DNA binding affinity dye, whereas dead cells with ruptured plasma membranes are stained with 7-AAD. Cells were fractionated into four groups, and live cells with depolarized mitochondrial membranes could be distinguished from those with intact mitochondrial membrane potential (Figure 2A). Treatment with 50 μM PIC increased the percentage of live cells with depolarized mitochondrial membranes (Figure 2A, B) and reduced live cells with intact mitochondrial membrane potential (Figure 2A and C). Cells with depolarized mitochondria were also increased by 30 μM PIC, whereas RSV at concentrations up to 50 μM had no effect on the mitochondrial membrane potential (Figure 2A-C). Thus, PIC, but not RSV, at a high

JPET Fast Forward. Published on December 17, 2020 as DOI: 10.1124/jpet.120.000096
This article has not been copyedited and formatted. The final version may differ from this version.

concentration affected mitochondrial membrane potential in C2C12 cells under our experimental conditions.

Induction of apoptosis by PIC, but not by RSV, at high concentrations

Depolarization of mitochondrial membrane potential leads to mitochondrial dysfunction and triggers cell death. We compared the effects of PIC and RSV on two types of cell death, apoptosis and necrosis. In this experiment, C2C12 cells were incubated with various concentrations of RSV or PIC for 4 h in serum-free DMEM. Apoptotic cell death was determined by condensed nuclei after nuclear staining (Figure 3A). Under the experimental conditions, RSV at concentrations up to 50 μM showed no cytotoxicity, whereas 30 and 50 μM PIC increased the number of cells with nuclear condensation (Figure 3A and B). Cytotoxicity of PIC and RSV was further analyzed by flow cytometry using Annexin V and 7-AAD, which detect apoptotic and necrotic cell death, respectively. The flow cytometric analysis fractionated cells into four fractions: live, early apoptotic, late apoptotic, and necrotic cells (Figure 3C). RSV at concentrations up to 50 μM did not increase apoptosis (Figure 3C, D and E). On the other hand, 50 μM PIC increased both early apoptosis and late apoptosis (Figure 3C, D and E). Necrosis was not increased by RSV or PIC (Figure 3F).

Effects of PIC on levels of mitochondrial ROS induced by antimycin A or H_2O_2

Although 50 μM PIC itself was cytotoxic (Figures 2 and 3), PIC had higher oxidant-scavenging ability than that of RSV (Figure 1), indicating the possibility that PIC at a low concentration has beneficial effects in cells with pathologically high levels of ROS. Since mitochondria are organelles that are a pathological source of ROS (Balaban et al., 2005; Bock and Tait, 2020), we compared the effects of PIC and RSV on levels of ROS directly generated from mitochondria by using antimycin A, an inhibitor of mitochondrial complex III.

Treatment of C2C12 cells with 30 μM RSV or PIC alone slightly increased the levels of MitoSOX Red fluorescence, an indicator of mitochondrial superoxide anion (Figure 4A and B). Treatment with antimycin A increased the fluorescence level of MitoSOX Red, which was suppressed by pretreatment with PIC or RSV (Figure 4A and B). PIC at 30 μM decreased MitoSOX Red fluorescence levels to approximately one-fourth of those in antimycin A-treated cells; however, 30 μM RSV reduced the levels of ROS only to three-quarters (Figure 4A and B). Thus, PIC achieved an approximately 3-fold decrease in the mitochondrial level of ROS compared with that achieved by RSV in cells treated with antimycin A.

The level of MitoSOX Red fluorescence was also increased by H_2O_2 (Figure 4C and D). RSV pretreatment reduced MitoSOX Red fluorescence level to approximately one-third of that in H_2O_2-treated cells. On the other hand, the H_2O_2-induced increase in MitoSOX Red fluorescence was almost completely suppressed by PIC (Figure 4C and D). Pretreatment with the same concentration of the anti-oxidative molecule vitamin C decreased the level of MitoSOX Red fluorescence to a level similar to that with RSV pretreatment. The other anti-oxidant NAC at 10 μM did not influence H_2O_2-induced MitoSOX Red fluorescence (Figure 4C and D).

Equal anti-necrotic activities of PIC and RSV

Mitochondrial ROS can induce necrotic cell death. Next, we examined the effects of 30 μM PIC and RSV on antimycin A-induced necrosis. To induce necrotic cell death, C2C12 cells were treated with a high concentration of antimycin A for 45 min and necrosis was monitored by flow cytometry after staining with 7-AAD. Neither PIC nor RSV alone affected necrosis (Supplemental Figure 2A and B). Antimycin A treatment increased the percentage of necrotic cells to 28.6% under the experimental conditions. Pretreatment with PIC and pretreatment with RSV decreased necrotic cell death induced by antimycin A to 23.2% and

JPET Fast Forward. Published on December 17, 2020 as DOI: 10.1124/jpet.120.000096
This article has not been copyedited and formatted. The final version may differ from this version.

23.4%, respectively (Supplemental Figure 2A and B). Thus, the potency of the anti-necrotic activity of PIC was similar to that of RSV.

Higher anti-apoptotic ability of PIC via SIRT1-dependent and -independent mechanisms

We compared the effects of PIC and RSV on apoptosis induced by antimycin A. To examine the involvement of SIRT1 in the anti-apoptotic function, SIRT1 was knocked down via siRNA. Treatment of cells with SIRT1 siRNA substantially reduced the SIRT1 protein level (Figure 5A) and SIRT1 knockdown alone did not affect apoptosis determined by nuclear condensation under this experimental condition (Figure 5B and C). Antimycin A increased the percentage of apoptotic cells to 44.3%. Pretreatment with either PIC or RSV suppressed antimycin A-induced apoptosis, and the reduction of apoptosis by PIC was greater than that by RSV. RSV at 10 μM reduced the percentage of apoptosis to 20.2% under the condition of antimycin A treatment (Figure 5B and C). On the other hand, in the presence of 10 μM PIC, the percentage of apoptotic cells was reduced to 10.4%. The anti-apoptotic effect of RSV was substantially suppressed by siRNA-mediated SIRT1 knockdown. In contrast, SIRT1 knockdown increased the percentage of apoptosis to 22.0% in cells treated with PIC (Figure 5B and C), suggesting that PIC protected the remaining approximately 20% of cells via mechanisms unrelated to SIRT1. The results indicated that PIC affords protection against mitochondrial ROS-induced cell death through SIRT1-dependent and -independent mechanisms.

Effects of SIRT1 and NRF2 on HO1 upregulation by PIC

PIC exerted more potent anti-oxidative and anti-apoptotic activities than those of RSV (Figures 4 and 5), and PIC decreased apoptotic cells via SIRT1-dependent and -independent

JPET Fast Forward. Published on December 17, 2020 as DOI: 10.1124/jpet.120.000096
This article has not been copyedited and formatted. The final version may differ from this version.

mechanisms (Figure 5). We compared the effects of PIC and RSV on induction of genes related to the anti-oxidative reaction regulated by SIRT1 and NRF2. The involvement of SIRT1 was also examined. RT-qPCR analysis confirmed SIRT1 knockdown by siRNA against SIRT1. Neither RSV nor PIC changed SIRT1 expression (Figure 6A). Among target genes of NRF2 examined in the present study, HO1 mRNA was upregulated by PIC but not by RSV. This upregulation was not affected by SIRT1 knockdown (Figure 6A). Levels of NQO1 and GCLM, the other targets of NRF2, were not changed by PIC or RSV. Although previous studies showed that RSV at a higher concentration upregulated SOD2, a target gene of FoxO transcription factors (Hori et al., 2013; Tanno et al., 2010), neither 10 μM RSV nor 10 μM PIC increased mRNA levels of SOD2 and catalase, another target of FoxOs (Figure 6A).

We further examined whether upregulation of HO1 by PIC is dependent on NRF2. Transfection of NRF2 siRNA reduced NRF2 mRNA levels by 83% of that in cells transfected with control siRNA, and neither RSV nor PIC changed the NRF2 mRNA level (Figure 6B). HO1 upregulation by PIC was blocked by NRF2 knockdown (Figure 6B). PIC slightly suppressed NQO1 and GCLM expression, and NRF2 knockdown further decreased the expression levels of these genes (Figure 6B). These results suggested that basal expression levels of these genes partly depend on NRF2.

Roles of heme oxygenase-1 in reductions in mitochondrial ROS level and apoptosis afforded by piceatannol

We examined whether HO1 is involved in the anti-oxidative and anti-apoptotic actions of PIC. HO1 level was effectively reduced by siRNA against HO1 (Figure 7A). PIC decreased the fluorescence level of MitoSOX Red induced by antimycin A to 24% of that in cells transfected with control siRNA without PIC. This ROS reduction by PIC was greater than that

JPET Fast Forward. Published on December 17, 2020 as DOI: 10.1124/jpet.120.000096
This article has not been copyedited and formatted. The final version may differ from this version.

by RSV (from 100% to 56%), being consistent with results shown in Figure 4. In the absence of antimycin A, HO1 knockdown alone did not change MitoSOX Red fluorescence. Compared with control siRNA cells, HO1 knockdown augmented antimycin A-induced increase in fluorescence level by 52% (Figure 7B and C). MitoSOX Red fluorescence level of cells treated with control siRNA was not affected by HO1 knockdown alone, but it was potentiated under the condition of antimycin A treatment (Figure 7B and C). HO1 siRNA treatment decreased the anti-oxidative function of PIC and RSV (Figure 7B and C). Although PIC decreased the fluorescence level of MitoSOX Red more than did RSV in cells treated with control siRNA, HO1 siRNA treatment cancelled the antioxidative function of PIC more than did RSV. Under the condition of HO1 knockdown, MitoSOX Red fluorescence level in PIC-treated cells was the same as than in cells treated with RSV (Figure 7B and C).

Apoptosis of cells transfected with control siRNA was not affected by HO1 knockdown in the absence of antimycin A (Figure 7D and E). HO1 siRNA did not affect the anti-apoptotic function of RSV, and RSV reduced the number of apoptotic cells in the presence of HO1 siRNA. In contrast to the effect of HO1 siRNA on RSV-treated cells, HO1 knockdown increased the number of apoptosis in PIC-treated cell and it completely abolished the anti-apoptotic function of PIC (Figure 7D and E).

Effects of RSV and PIC on myotube differentiation of C2C12 myoblasts

Finally, we examined the effects of RSV and PIC on the differentiation of C2C12 cells because RSV has been reported to promote differentiation of C2C12 myoblast cells (Montesano et al. 2013). Treatment of cells with a differentiation medium containing 2% horse serum for 7 days changed the shape of cells and myotubes were formed (Supplemental Figure 3A). Levels of myogenin and myosin heavy chain 4 (MYH4) mRNAs were increased by the differentiation medium although the expression of MyoD, a master transcription factor

JPET Fast Forward. Published on December 17, 2020 as DOI: 10.1124/jpet.120.000096
This article has not been copyedited and formatted. The final version may differ from this version.

of myogenesis, was not changed (Supplemental Figure 3B). The addition of RSV or PIC to the differentiation medium did not affect the appearance of cells (Supplemental Figure 3A). RSV and PIC did not affect myogenin and MyoD mRNA levels, but RSV or PIC treatment enhanced the expression levels of MYH4 (Supplemental Figure 3B). The magnitude of the increase in MYH4 expression induced by RSV was greater than that induced by PIC (Supplemental Figure 3B).

Discussion

Under the condition of treatment of cells with antimycin A or H_2O_2, PIC reduced mitochondrial ROS and apoptotic cells more than did RSV (Figures 4 and 5). These findings indicate that cytoprotection by PIC is more potent than that by RSV against mitochondrial ROS. The reduction in apoptosis by RSV was mostly dependent on SIRT1, while the involvement of SIRT1 in PIC's anti-apoptotic action was partial (Figure 5). In contrast, PIC, but not RSV, upregulated HO1, which was blocked by NRF2 knockdown but not by SIRT1 knockdown (Figure 6). HO1 knockdown abolished the effects of PIC on mitochondrial ROS and apoptosis but had no influence on the effects of RSV (Figure 7). These findings suggest that the cytoprotecion by PIC is mainly attributed to HO1 induction via NRF2 activation.

PIC was detected in the intracellular fraction of cells treated with PIC (Supplemental Figure 1), and an additional peak was not detected. These suggested that PIC entered cells without metabolic modifications. It also means that PIC can reach intracellular targets including NRF2 and SIRT1 to exert its functions. In addition, it is unlikely that we would detect PIC bound to the outer side of the plasma membrane because PIC was not detected in the intracellular fraction from cells harvested after PIC incubation for 1 min (Supplemental Figure 1).

JPET Fast Forward. Published on December 17, 2020 as DOI: 10.1124/jpet.120.000096
This article has not been copyedited and formatted. The final version may differ from this version.

Oxidation or covalent modification of thiol groups of Keap1 disrupts its repression of NRF2, resulting in NRF2 translocation to the nucleus (Yamamoto et al., 2018). Lee et al. hypothesized that cysteine residues of Keap1 are targets of PIC for its NRF2 activation and showed that HO1 induction by PIC was blocked by thiol reducing agents (Lee et al., 2010). The authors speculated that PIC directly interacts with a critical thiol(s) of Keap1 because the catechol structure of PIC is likely to be oxidized to form quinone, which targets cysteine thiols. Another compound with a catechol structure had also been reported to be oxidized to quinone, which binds to thiol groups of Keap1 (Sumi et al., 2009). Since RSV does not have a catechol structure, such a structural difference may explain why RSV did not activate NRF2.

In cells treated with H_2O_2, the reduction in MitoSox Red fluorescence levels by PIC was greater than that by RSV or vitamin C (Figure 4C and D). Our data suggest that this powerful ROS-reducing function of PIC is derived from both its radical scavenging property (Figure 1) and HO1 induction (Figure 7). However, the radical scavenging activity of piceatannol itself seems to play a minor role in cytoprotection by PIC because knockdown of HO1 almost completely abolished the anti-apoptotic effect of PIC.

HO1 is tethered to the membrane of the endoplasmic reticulum (Dunn et al., 2014). Free heme promotes the formation of a cytotoxic hydroxy radical from H_2O_2 through the Fenton reaction. HO1 catabolizes free heme into Fe^{2+}, carbon monoxide, and biliverdin (Gozzelino et al., 2010). Bilirubin converted from biliverdin by biliverdin reductase exerts anti-oxidant activity (Gozzelino et al., 2010). Interestingly, it has been reported that HO1 and biliverdin reductase localize in the mitochondria of the rat liver, where HO1 reduces mitochondrial heme content (Converso et al., 2006). Furthermore, HO1 translocates to mitochondria in response to mitochondrial oxidative stress in gastric mucosal cells, resulting in protection from mitochondrial damage and apoptosis (Bindu et al., 2011). Therefore, upregulated HO1

by PIC might have located in the mitochondria and reduced mitochondrial ROS and apoptosis.

Anti-apoptotic actions of RSV and PIC were attenuated by SIRT1 knockdown (Figure 5). However, RSV and PIC failed to induce SOD2 and catalase, which are target genes of FoxOs activated by SIRT1, probably because of a lower dose of RSV than the doses used in previous studies (Hori et al., 2013; Tanno et al., 2010). As a possible SIRT1-dependent protective mechanism, we previously reported that knockdown of the transcription factor p53, a deacetylation target of SIRT1, reduced antimycin A-induced apoptosis in C2C12 cells and that treatment of cells with RSV reduced the level of acetyl-p53 (Hori et al., 2013). Since deacetylation of p53 by SIRT1 negatively regulates p53 activity (Luo et al., 2001), inhibition of p53 may be involved in the SIRT1-mediated anti-apoptotic actions of RSV and PIC. In addition, we reported that activation of autophagy/mitophagy is involved in the decrease in mitochondrial ROS by RSV in C2C12 cells (Sebori et al., 2018). Elimination of damaged mitochondria via mitophagy may also play a role in the reduction of ROS by RSV and the anti-apoptotic action of RSV.

RSV at a higher concentration did not affect mitochondrial membrane potential and apoptosis in C2C12 cells (Figures 2 and 3), although administration of RSV at more than 2 g/day in humans often causes gastrointestinal symptoms such as diarrhea and abdominal pain (Patel et al., 2011). On the other hand, PIC promoted mitochondrial membrane depolarization and induced apoptosis at higher concentrations (Figures 2 and 3). PIC has high anti-cancer activity for various tumors (Piotrowska et al., 2012). Numerous mechanisms of the anti-cancer activity of PIC have been reported. The reported mechanisms include activation of caspases, inhibition of Janus kinase, down-regulation of cell cycle inducers, activation of poly (ADP-ribose) polymerase, decrease of Bcl-2 and Bcl-X_L, upregulation of Fas and FasL, inhibition of mitochondrial F_1-ATPase, and inhibition of ribonuclease reductase (Piotrowska

et al., 2012; Seyed et al., 2016; Wieder et al., 2001). Experimental conditions including cell types, concentration of PIC, and treatment duration were different in previous studies. However, a relatively high concentration of PIC (i.e., 50 μM) was used in most studies for analyses of anti-tumor effects. Nevertheless, it is important to pay attention to the optimum therapeutic dose of PIC when we apply PIC to cytoprotection against cellular insult such as oxidative stress.

Although there has been no study on the pharmacokinetics of PIC in humans, a study using rats showed that PIC possesses higher metabolic stability than that of RSV (Setoguchi et al., 2014). The elimination half-life of PIC after intravenous administration was 313 min, and PIC was still detected 12 h after administration (Roupe et al., 2004). On the other hand, RSV is subjected to rapid and extensive metabolism after oral administration (Walle et al., 2004), and the elimination half-life of RSV was quite rapid and less than 3 h in humans (Almeida et al., 2009; Kawamura et al., 2020). Although PIC and RSV are nonspecific compounds and target various molecules, both of them have been shown to have therapeutic potentials (Bonkowski and Sinclair, 2016; Piotrowska et al., 2012; Salehi et al., 2018; Seyed et al., 2016). The results of those studies and the present study suggest that PIC is an alternative and promising agent for treatment of various diseases in which ROS are strongly involved, though further studies regarding the safety and pharmacokinetics of PIC in humans are required.

Acknowledgments.

None.

Authorship Contributions.

Participated in research design: Hosoda, Hamada, Horio, Kuno

Conducted experiments: Hosoda, Uesugi, Iwahara, Nojima

Performed data analysis: Hosoda, Hamada, Iwahara, Nojima, Horio, Kuno

Wrote or contributed to the writing of the manuscript: Hosoda, Horio, Kuno

References.

Almeida L, Vaz-da-Silva M, Falcao A, Soares E, Costa R, Loureiro AI, Fernandes-Lopes C, Rocha JF, Nunes T, Wright L and Soares-da-Silva P (2009) Pharmacokinetic and safety profile of trans-resveratrol in a rising multiple-dose study in healthy volunteers. *Mol Nutr Food Res* **53 Suppl 1**:S7-15.

Balaban RS, Nemoto S and Finkel T (2005) Mitochondria, oxidants, and aging. *Cell* **120**:483-495.

Bindu S, Pal C, Dey S, Goyal M, Alam A, Iqbal MS, Dutta S, Sarkar S, Kumar R, Maity P and Bandyopadhyay U (2011) Translocation of heme oxygenase-1 to mitochondria is a novel cytoprotective mechanism against non-steroidal anti-inflammatory drug-induced mitochondrial oxidative stress, apoptosis, and gastric mucosal injury. *J Biol Chem* **286**:39387-39402.

Bock FJ and Tait SWG (2020) Mitochondria as multifaceted regulators of cell death. *Nat Rev Mol Cell Biol* **21**:85-100.

Bonkowski MS and Sinclair DA (2016) Slowing ageing by design: the rise of NAD(+) and sirtuin-activating compounds. *Nat Rev Mol Cell Biol* **17**:679-690.

Converso DP, Taille C, Carreras MC, Jaitovich A, Poderoso JJ and Boczkowski J (2006) HO-1 is located in liver mitochondria and modulates mitochondrial heme content and metabolism. *FASEB J* **20**:1236-1238.

Cuadrado A, Rojo AI, Wells G, Hayes JD, Cousin SP, Rumsey WL, Attucks OC, Franklin S, Levonen AL, Kensler TW and Dinkova-Kostova AT (2019) Therapeutic targeting of the NRF2 and KEAP1 partnership in chronic diseases. *Nat Rev Drug Discov* **18**:295-317.

Dunn LL, Midwinter RG, Ni J, Hamid HA, Parish CR and Stocker R (2014) New insights into intracellular locations and functions of heme oxygenase-1. *Antioxid Redox Signal*

20:1723-1742.

Fujiwara D, Iwahara N, Sebori R, Hosoda R, Shimohama S, Kuno A and Horio Y (2019) SIRT1 deficiency interferes with membrane resealing after cell membrane injury. *PLoS One* **14**:e0218329.

Gozzelino R, Jeney V and Soares MP (2010) Mechanisms of cell protection by heme oxygenase-1. *Annu Rev Pharmacol Toxicol* **50**:323-354.

Hao E, Lang F, Chen Y, Zhang H, Cong X, Shen X and Su G (2013) Resveratrol alleviates endotoxin-induced myocardial toxicity via the Nrf2 transcription factor. *PLoS One* **8**:e69452.

Hori YS, Kuno A, Hosoda R and Horio Y (2013) Regulation of FOXOs and p53 by SIRT1 modulators under oxidative stress. *PLoS One* **8**:e73875.

Horio Y, Hayashi T, Kuno A and Kunimoto R (2011) Cellular and molecular effects of sirtuins in health and disease. *Clin Sci (Lond)* **121**:191-203.

Hosoda R, Kuno A, Hori YS, Ohtani K, Wakamiya N, Oohiro A, Hamada H and Horio Y (2013) Differential cell-protective function of two resveratrol (trans-3,5,4'-trihydroxystilbene) glucosides against oxidative stress. *J Pharmacol Exp Ther* **344**:124-132.

Howitz KT, Bitterman KJ, Cohen HY, Lamming DW, Lavu S, Wood JG, Zipkin RE, Chung P, Kisielewski A, Zhang LL, Scherer B and Sinclair DA (2003) Small molecule activators of sirtuins extend Saccharomyces cerevisiae lifespan. *Nature* **425**:191-196.

Huang K, Huang J, Xie X, Wang S, Chen C, Shen X, Liu P and Huang H (2013) Sirt1 resists advanced glycation end products-induced expressions of fibronectin and TGF-beta1 by activating the Nrf2/ARE pathway in glomerular mesangial cells. *Free Radic Biol Med* **65**:528-540.

Jang YJ, Kim JE, Kang NJ, Lee KW and Lee HJ (2009) Piceatannol attenuates

4-hydroxynonenal-induced apoptosis of PC12 cells by blocking activation of c-Jun N-terminal kinase. *Ann N Y Acad Sci* **1171**:176-182.

Kaeberlein M, McVey M and Guarente L (1999) The SIR2/3/4 complex and SIR2 alone promote longevity in Saccharomyces cerevisiae by two different mechanisms. *Genes Dev* **13**:2570-2580.

Kawai Y, Garduno L, Theodore M, Yang J and Arinze IJ (2011) Acetylation-deacetylation of the transcription factor Nrf2 (nuclear factor erythroid 2-related factor 2) regulates its transcriptional activity and nucleocytoplasmic localization. *J Biol Chem* **286**:7629-7640.

Kawamura K, Fukumura S, Nikaido K, Tachi N, Kozuka N, Seino T, Hatakeyama K, Mori M, Ito YM, Takami A, Hinotsu S, Kuno A, Kawasaki Y, Horio Y and Tsutsumi H (2020) Resveratrol improves motor function in patients with muscular dystrophies: an open-label, single-arm, phase IIa study. *Sci Rep* **10**:20585.

Kim HJ, Lee KW and Lee HJ (2007) Protective effects of piceatannol against beta-amyloid-induced neuronal cell death. *Ann N Y Acad Sci* **1095**:473-482.

Kuno A, Hosoda R, Sebori R, Hayashi T, Sakuragi H, Tanabe M and Horio Y (2018) Resveratrol Ameliorates Mitophagy Disturbance and Improves Cardiac Pathophysiology of Dystrophin-deficient mdx Mice. *Sci Rep* **8**:15555.

Lee HH, Park SA, Almazari I, Kim EH, Na HK and Surh YJ (2010) Piceatannol induces heme oxygenase-1 expression in human mammary epithelial cells through activation of ARE-driven Nrf2 signaling. *Arch Biochem Biophys* **501**:142-150.

Lee J, Giordano S and Zhang J (2012) Autophagy, mitochondria and oxidative stress: cross-talk and redox signalling. *Biochem J* **441**:523-540.

Luo J, Nikolaev AY, Imai S, Chen D, Su F, Shiloh A, Guarente L and Gu W (2001) Negative control of p53 by Sir2alpha promotes cell survival under stress. *Cell* **107**:137-148.

Morales FJ and Jimenez-Perez S (2001) Free radical scavenging capacity of Maillard reaction products as related to colour and fluorescence. *Food Chem* **72**:119-125.

Morselli E, Marino G, Bennetzen MV, Eisenberg T, Megalou E, Schroeder S, Cabrera S, Benit P, Rustin P, Criollo A, Kepp O, Galluzzi L, Shen S, Malik SA, Maiuri MC, Horio Y, Lopez-Otin C, Andersen JS, Tavernarakis N, Madeo F and Kroemer G (2011) Spermidine and resveratrol induce autophagy by distinct pathways converging on the acetylproteome. *J Cell Biol* **192**:615-629.

Pan H and Finkel T (2017) Key proteins and pathways that regulate lifespan. *J Biol Chem* **292**:6452-6460.

Patel KR, Scott E, Brown VA, Gescher AJ, Steward WP and Brown K (2011) Clinical trials of resveratrol. *Ann N Y Acad Sci* **1215**:161-169.

Perez-Leal O, Barrero CA and Merali S (2017) Pharmacological stimulation of nuclear factor (erythroid-derived 2)-like 2 translation activates antioxidant responses. *J Biol Chem* **292**:14108-14121.

Piotrowska H, Kucinska M and Murias M (2012) Biological activity of piceatannol: leaving the shadow of resveratrol. *Mutat Res* **750**:60-82.

Rhayem Y, Therond P, Camont L, Couturier M, Beaudeux JL, Legrand A, Jore D, Gardes-Albert M and Bonnefont-Rousselot D (2008) Chain-breaking activity of resveratrol and piceatannol in a linoleate micellar model. *Chem Phys Lipids* **155**:48-56.

Roupe K, Teng XW, Fu X, Meadows GG and Davies NM (2004) Determination of piceatannol in rat serum and liver microsomes: pharmacokinetics and phase I and II biotransformation. *Biomed Chromatogr* **18**:486-491.

Sakamoto J, Miura T, Shimamoto K and Horio Y (2004) Predominant expression of Sir2alpha, an NAD-dependent histone deacetylase, in the embryonic mouse heart and brain.

FEBS Lett **556**:281-286.

Salehi B, Mishra AP, Nigam M, Sener B, Kilic M, Sharifi-Rad M, Fokou PVT, Martins N and Sharifi-Rad J (2018) Resveratrol: A Double-Edged Sword in Health Benefits. *Biomedicines* **6**.

Sato D, Shimizu N, Shimizu Y, Akagi M, Eshita Y, Ozaki S, Nakajima N, Ishihara K, Masuoka N, Hamada H, Shimoda K and Kubota N (2014) Synthesis of glycosides of resveratrol, pterostilbene, and piceatannol, and their anti-oxidant, anti-allergic, and neuroprotective activities. *Biosci Biotechnol Biochem* **78**:1123-1128.

Sebori R, Kuno A, Hosoda R, Hayashi T and Horio Y (2018) Resveratrol Decreases Oxidative Stress by Restoring Mitophagy and Improves the Pathophysiology of Dystrophin-Deficient mdx Mice. *Oxid Med Cell Longev* **2018**:9179270.

Setoguchi Y, Oritani Y, Ito R, Inagaki H, Maruki-Uchida H, Ichiyanagi T and Ito T (2014) Absorption and metabolism of piceatannol in rats. *J Agric Food Chem* **62**:2541-2548.

Seyed MA, Jantan I, Bukhari SN and Vijayaraghavan K (2016) A Comprehensive Review on the Chemotherapeutic Potential of Piceatannol for Cancer Treatment, with Mechanistic Insights. *J Agric Food Chem* **64**:725-737.

Sueishi Y, Nii R and Kakizaki N (2017) Resveratrol analogues like piceatannol are potent antioxidants as quantitatively demonstrated through the high scavenging ability against reactive oxygen species and methyl radical. *Bioorg Med Chem Lett* **27**:5203-5206.

Sumi D, Numasawa Y, Endo A, Iwamoto N and Kumagai Y (2009) Catechol estrogens mediated activation of Nrf2 through covalent modification of its quinone metabolite to Keap1. *J Toxicol Sci* **34**:627-635.

Sun Z, Chin YE and Zhang DD (2009) Acetylation of Nrf2 by p300/CBP augments promoter-specific DNA binding of Nrf2 during the antioxidant response. *Mol Cell Biol*

29:2658-2672.

Tanno M, Kuno A, Yano T, Miura T, Hisahara S, Ishikawa S, Shimamoto K and Horio Y (2010) Induction of manganese superoxide dismutase by nuclear translocation and activation of SIRT1 promotes cell survival in chronic heart failure. *J Biol Chem* **285**:8375-8382.

Veith A and Moorthy B (2018) Role of Cytochrome P450s in the Generation and Metabolism of Reactive Oxygen Species. *Curr Opin Toxicol* **7**:44-51.

Walle T, Hsieh F, DeLegge MH, Oatis JE, Jr. and Walle UK (2004) High absorption but very low bioavailability of oral resveratrol in humans. *Drug Metab Dispos* **32**:1377-1382.

Wieder T, Prokop A, Bagci B, Essmann F, Bernicke D, Schulze-Osthoff K, Dorken B, Schmalz HG, Daniel PT and Henze G (2001) Piceatannol, a hydroxylated analog of the chemopreventive agent resveratrol, is a potent inducer of apoptosis in the lymphoma cell line BJAB and in primary, leukemic lymphoblasts. *Leukemia* **15**:1735-1742.

Yamamoto M, Kensler TW and Motohashi H (2018) The KEAP1-NRF2 System: a Thiol-Based Sensor-Effector Apparatus for Maintaining Redox Homeostasis. *Physiol Rev* **98**:1169-1203.

Zhang Y, Murugesan P, Huang K and Cai H (2020) NADPH oxidases and oxidase crosstalk in cardiovascular diseases: novel therapeutic targets. *Nat Rev Cardiol* **17**:170-194.

Footnotes.

This work was supported in part by a research grants from the Chugoku Regional Innovation Research Center (H. H., Y. H), the Hiroshige Kondo Foundation (Y.H.), and Grants-in-Aid for Regional R&D Proposal-Based Program from Northern Advancement Center for Science & Technology of Hokkaido Japan.

Conflicts of interest.

All authors have no conflicts of interest to declare.

JPET Fast Forward. Published on December 17, 2020 as DOI: 10.1124/jpet.120.000096
This article has not been copyedited and formatted. The final version may differ from this version.

Figure legends.

Figure 1. Chemical structures and in vitro antioxidant activity of resveratrol and piceatannol.

(A) Chemical structures of resveratrol and piceatannol. (B) The DPPH radical-scavenging activity of PIC and RSV. Data were obtained from three independent experiments. *P < 0.05.

Figure 2. Effects of piceatannol and resveratrol on mitochondrial depolarization in C2C12 cells.

(A) C2C12 cells were treated with resveratrol (RSV) or piceatannol (PIC) at 0, 10, 30, and 50 μM for 4 h, stained with MitoPotential Dye and 7-Amino-Actinomycin D (7-AAD), and analyzed by flow cytometry. Cells were fractionated into four groups according to the manufacturer's protocol; live cells with intact mitochondrial membrane potential, MitoPotential Dye (+) and 7-AAD (-); depolarized live cells, MitoPotential Dye (-) and 7-AAD (-); depolarized dead cells, MitoPotential Dye (-) and 7-AAD (+); and dead cells, MitoPotential Dye (+) and 7-AAD (+). The percentages of live cells with depolarized mitochondria (B) and live cells with intact mitochondrial membrane potential (C) were shown. One-way ANOVA followed by a Student-Neuman-Keuls test was performed to analyze the statistical difference. n = 6, *P < 0.05.

Figure 3. Effects of piceatannol and resveratrol on cell death in C2C12 cells.

C2C12 cells were treated with resveratrol (RSV) or piceatannol (PIC) at 0, 10, 30, and 50 μM for 4 h, and then cells were stained with Hoechst33342 (A, B) or analyzed by flow cytometry (C-F). (A) Representative images of nuclear staining with Hoechst33342 in C2C12 cells. An arrow indicates a condensed nucleus, an index of apoptosis. Scale bar: 50 μm. (B) Summary data of the percentages of cells with nuclear condensation. The mean percentage of apoptotic

cells was obtained from 5 fields for each treatment, and data from three independent experiments were analyzed. One-way ANOVA followed by a Student-Neuman-Keuls test was performed to analyze the statistical difference. *P < 0.05. (C) Representative profiles of cells stained with Annexin V and 7-AAD. Cells were fractionated into four fractions: live cells, Annexin V (-) and 7-AAD (-); early apoptotic cells, Annexin V (+) and 7-AAD (-); late apoptotic cells, Annexin V (+) and 7-AAD (+); and necrotic cells, Annexin V (-) and 7-AAD (+). The percentages of cells with early apoptosis (D), late apoptosis (E), and necrosis (F) are shown. One-way ANOVA followed by a Student-Neuman-Keuls test was performed to analyze the statistical difference. n = 4. *P < 0.05. NS; not significant.

Figure 4. Effects of piceatannol and resveratrol on mitochondrial levels of ROS induced by antimycin A or H_2O_2.

(A) Representative images of MitoSOX Red fluorescence in C2C12 cells treated with a vehicle, 30 μM resveratrol (RSV) or 30 μM piceatannol (PIC) for 4 h and then stimulated with a vehicle or 45 μM antimycin A (AA) for 4 h under a serum-free condition. (B) Mean level of MitoSOX Red fluorescence intensity in each treatment. Scale bar: 100 μm. The average fluorescence intensity was obtained from 6 fields for each experiment, and the data from 3 independent experiments were analyzed. (C) Representative images of MitoSOX Red fluorescence in cells pretreated with a vehicle, 10 μM RSV, 10 μM PIC, 10 μM vitamin C (VC), or 10 μM N-acetyl-L-cysteine (NAC) for 24 h followed by co-incubation of a vehicle or 250 μM H_2O_2 for 1 h. (D) Summary data of MitoSOX Red fluorescence. The average of MitoSOX florescence per cell was obtained from randomly selected 5 fields for each experiment, and the data from 3 independent experiments were analyzed. One-way ANOVA followed by a Student-Neuman-Keuls test was performed to analyze the statistical difference among groups. *P < 0.05. a.u.; arbitrary unit.

JPET Fast Forward. Published on December 17, 2020 as DOI: 10.1124/jpet.120.000096
This article has not been copyedited and formatted. The final version may differ from this version.

Figure 5. The role of SIRT1 in anti-apoptotic effects of piceatannol and resveratrol.

(A) (Upper) Representative immunoblots for SIRT1 and α-tubulin in C2C12 cells transfected with control siRNA or SIRT1 siRNA. (Lower) Relative expression levels of SIRT1 protein normalized by α-tubulin level. n=3. *P < 0.05 by two-tailed unpaired t-test. (B) C2C12 cells transfected with either control siRNA or SIRT1 siRNA were pretreated with a vehicle, 10 μM piceatannol (PIC), or 10 μM resveratrol (RSV) for 24 h and then treated with 30 μM antimycin A (AA) for 4 h to induce apoptosis in a serum-free condition. Cells were stained by Hoechst33342 and nuclear condensation was examined. Representative images of nuclear staining with Hoechst33342. An arrow indicates a condensed nucleus, a marker of apoptosis. Scale bar: 100 μm. (C) Percentage of apoptotic cells in each treatment. The average of the percentage of apoptotic cells was obtained from 5 fields for each treatment, and the data from 3 independent experiments were analyzed. Two-way ANOVA followed by a Student-Neuman-Keuls test was performed to analyze the statistical difference among groups. *P < 0.05. NS; not significant.

Figure 6. Roles of SIRT1 and NRF2 in effects of piceatannol and resveratrol on changes in expression of genes related to anti-oxidative reaction.

(A) C2C12 cells were treated with a vehicle (Control), 10 μM resveratrol (RSV), or 10 μM piceatannol (PIC) for 24 h under a serum-free condition after transfection of control or SIRT1 siRNA. SIRT1, HO1, NQO1, GCLM, SOD2, and catalase mRNA levels were measured by a quantitative PCR method. N= 4. (B) Cells were treated with the vehicle, RSV, or PIC as in (A) after transfection of control or NRF2 siRNA. Levels of NRF2, HO1, NQO1, and GCLM mRNA were analyzed. N=3. Two-way ANOVA followed by a Student-Neuman-Keuls test

JPET Fast Forward. Published on December 17, 2020 as DOI: 10.1124/jpet.120.000096
This article has not been copyedited and formatted. The final version may differ from this version.

was performed to analyze the statistical difference among groups. *P < 0.05. NS; not significant.

Figure 7. The involvement of heme oxygenase-1 in reductions in mitochondrial ROS and apoptosis afforded by PIC.

(A) HO1 mRNA levels normalized to GAPDH in C2C12 cells transfected with control or HO1 siRNA. (B) Representative images of MitoSOX Red fluorescence. Scale bar: 100 μm. Cells were transfected with control- or HO1-siRNA and were then pretreated with a vehicle, 10 μM resveratrol (RSV), or 10 μM piceatannol (PIC) for 24 h under a serum-free condition. Cells were stimulated with 30 μM antimycin A (AA) for 1 h to produce mitochondrial ROS which was analyzed using MitoSOX Red. (C) Average of intensity of MitoSOX Red fluorescence per cell. Randomly selected 15 fields from independent 3 experiments were analyzed. (D) Representative images of nuclear staining with Hoechst33342. An arrow indicates a condensed nucleus, a marker of apoptosis. Scale bar: 100 μm. (E) The average of the percentage of cells with condensed nuclei. Randomly selected 15 fields from independent 3 experiments were analyzed. Two-way ANOVA followed by a Student-Neuman-Keuls test was performed to analyze the statistical difference among groups in (C) and (E). *P < 0.05.

Fig. 1

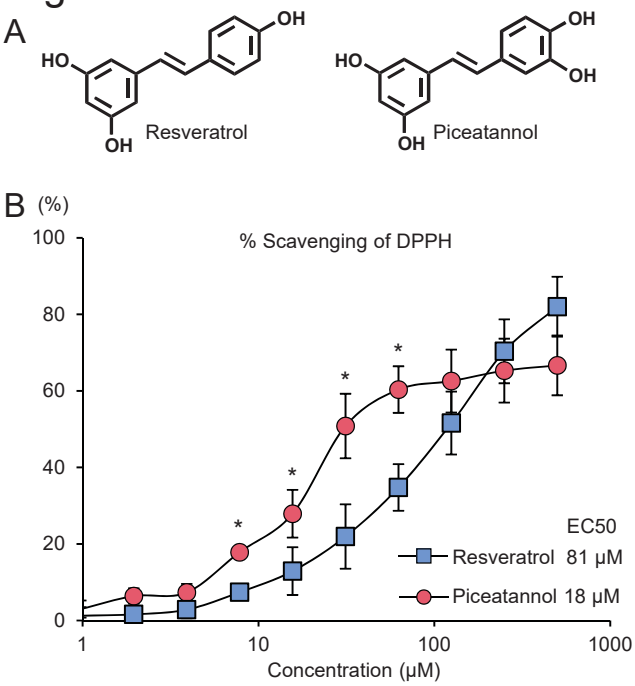

Fig. 2

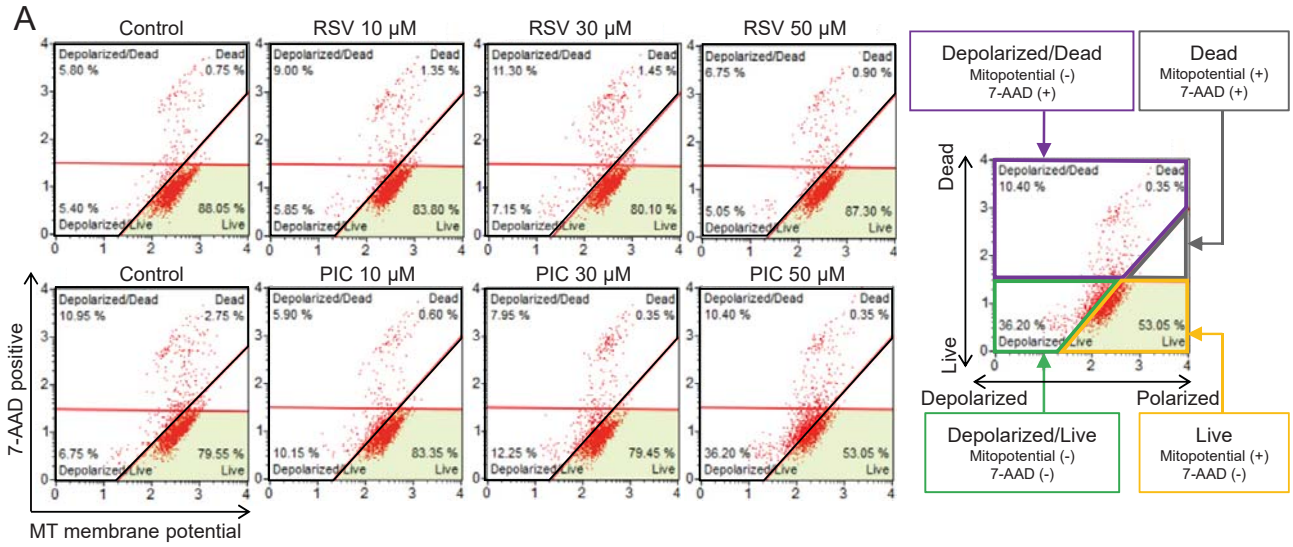

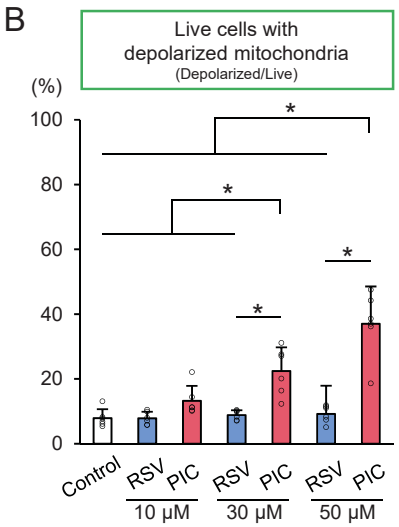

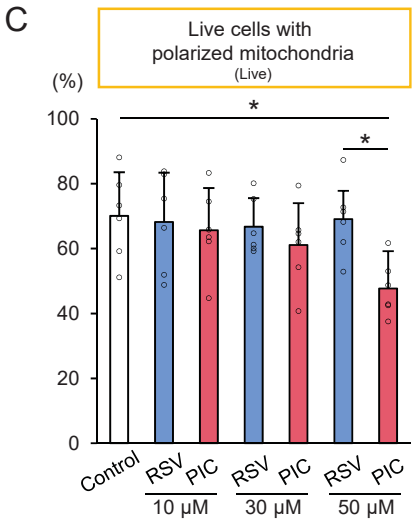

Fig. 3

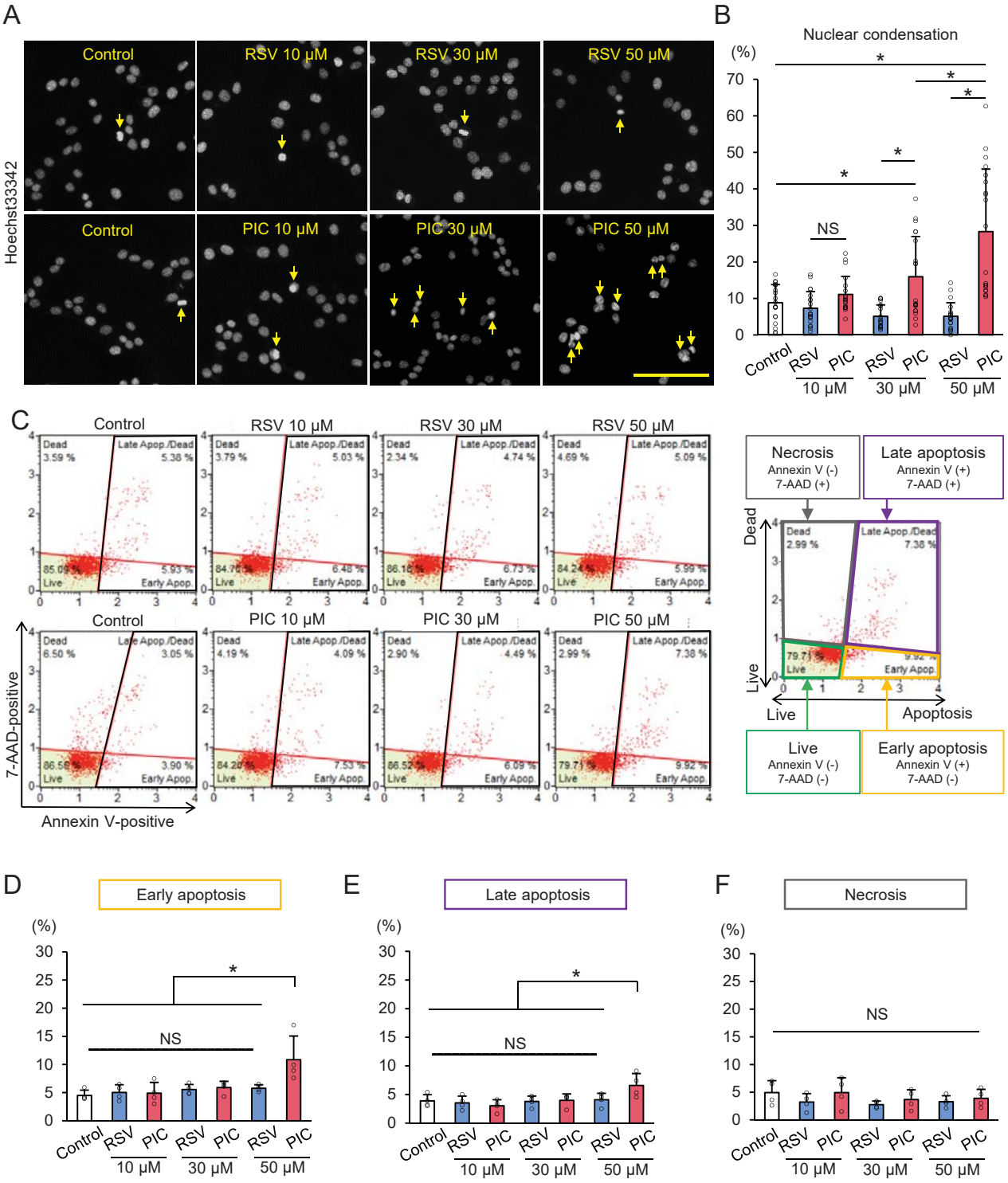

Fig. 4

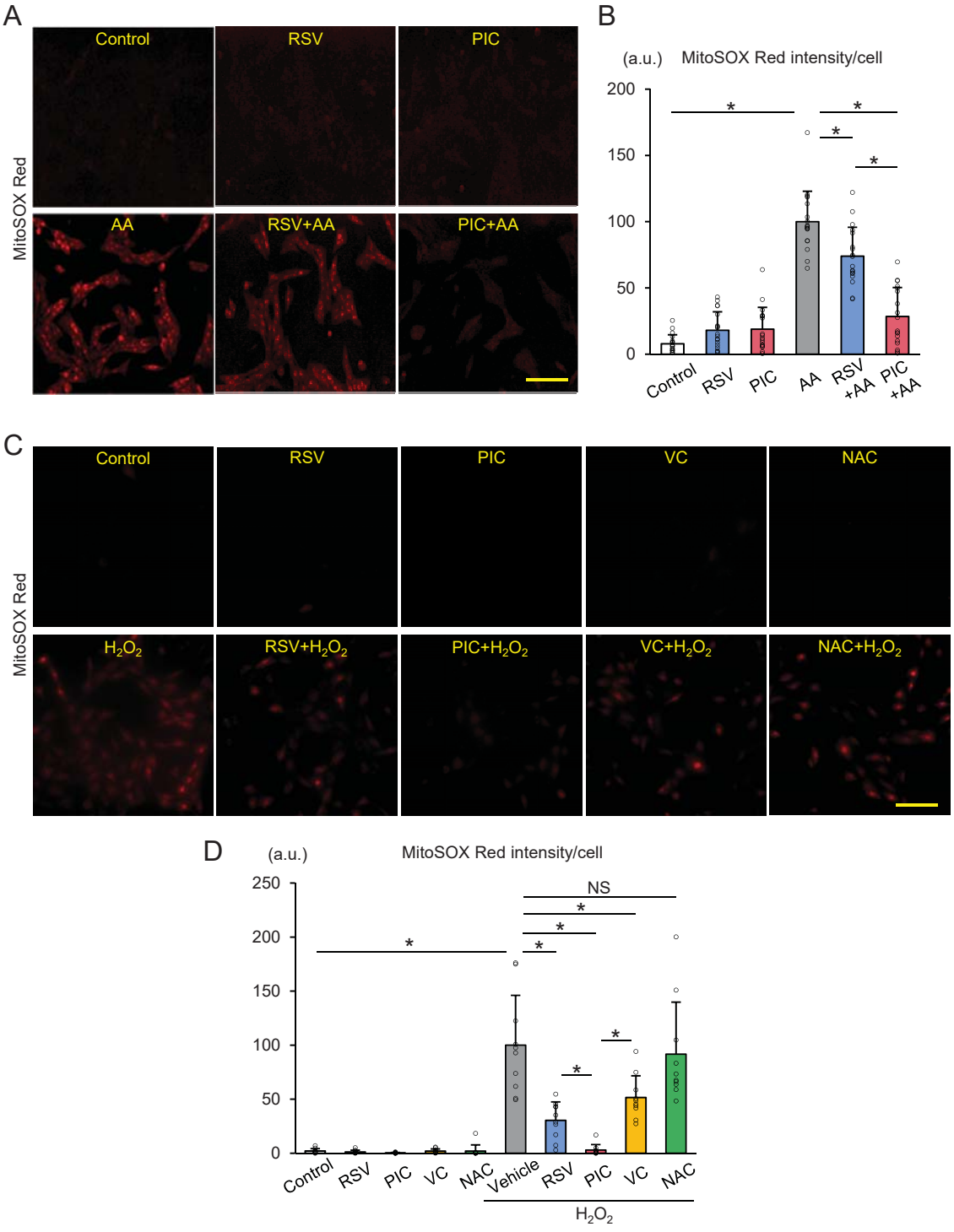

Fig. 5

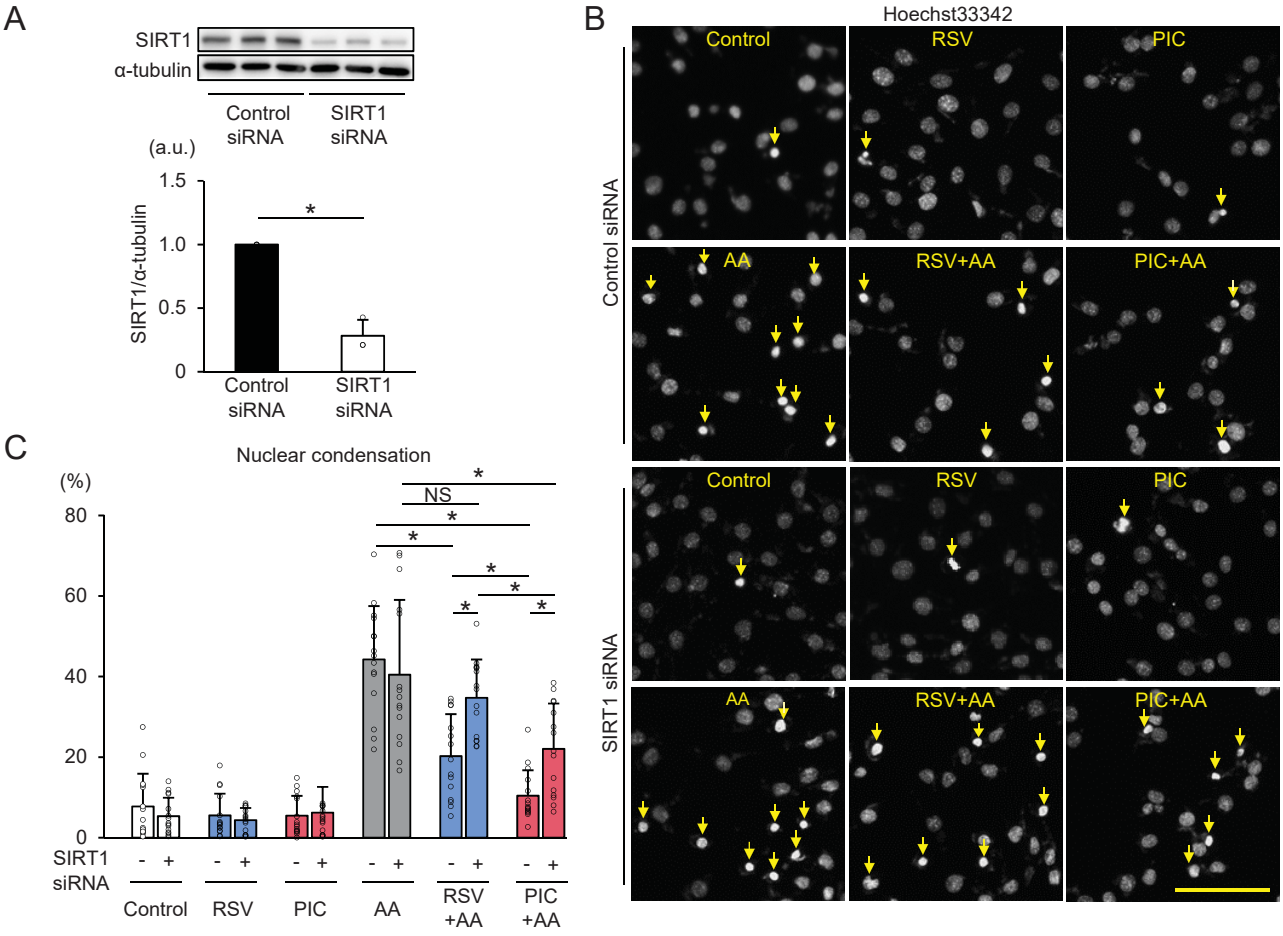

Fig. 6

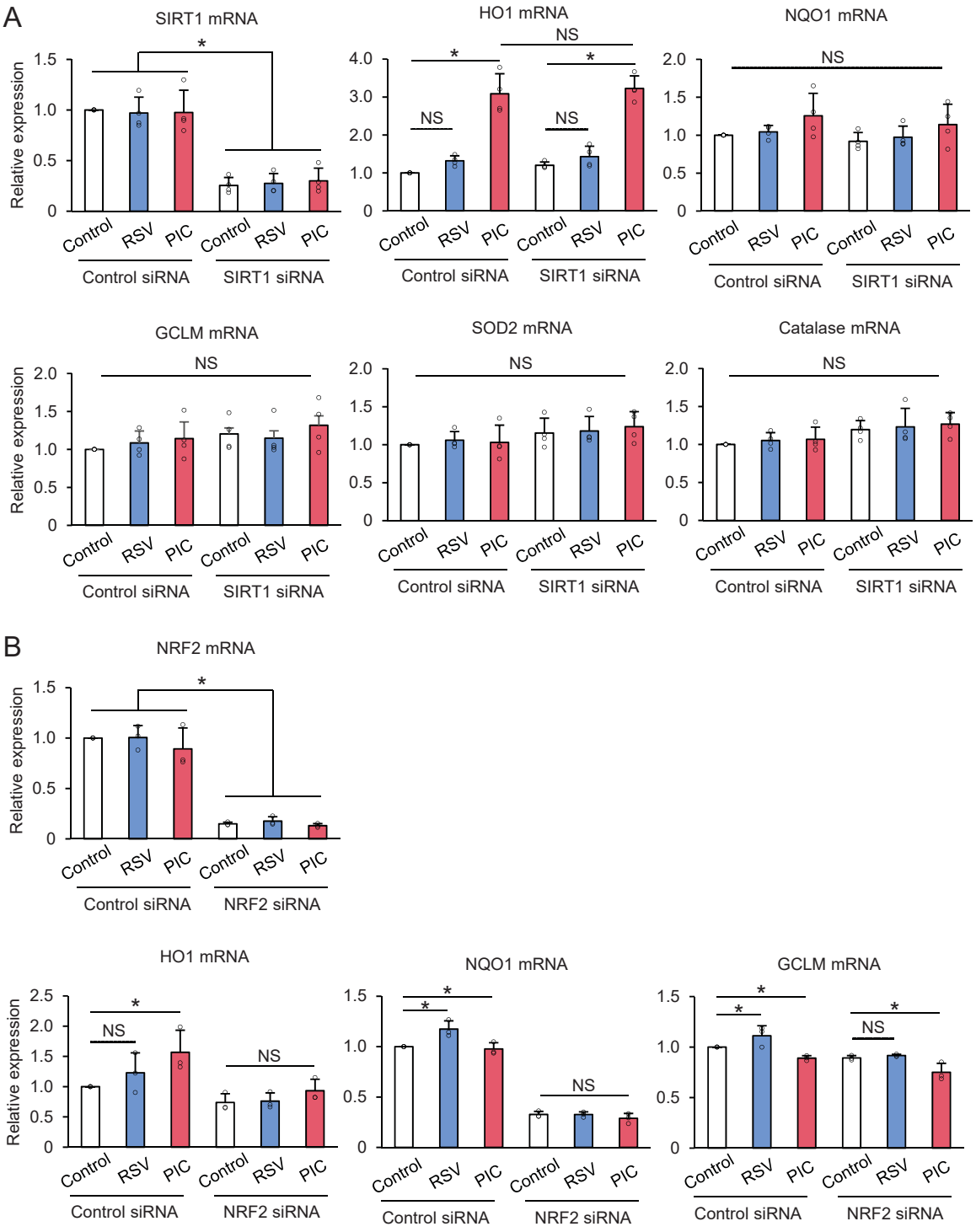

JPET Fast Forward. Published on December 17, 2020 as DOI: 10.1124/jpet.120.000096
This article has not been copyedited and formatted. The final version may differ from this version.

Fig. 7